

**TRANSONIC AXIAL-FLOW BLADE SHAPE OPTIMIZATION
USING EVOLUTIONARY ALGORITHM
AND THREE-DIMENSIONAL NAVIER-STOKES SOLVER**

Akira Oyama*

NASA Glenn Research Center, Brook Park, OH 44135, USA
(440) 962-3148, akiraoyama@dino.grc.nasa.gov

and

Meng-Sing Liou†

NASA Glenn Research Center, MS 5-11, Brook Park, OH 44135, USA
(216) 433-5855, meng-sing.liou@grc.nasa.gov

and

Shigeru Obayashi#

Tohoku University, Katahira 2-1-1, Sendai, Japan
+81-22-217-5265, obayashi@ieee.org

ABSTRACT

A reliable and efficient aerodynamic design optimization tool using evolutionary algorithm has been developed for transonic compressor blades. A real-coded adaptive-range genetic algorithm is used to improve efficiency and robustness in design optimization. To represent flow fields accurately and produce reliable designs, three-dimensional Navier-Stokes computation is used for aerodynamic analysis.

To ensure feasibility of the present method, aerodynamic redesign of NASA rotor67 is demonstrated. Entropy production is considered as the objective function to be minimized. The computation is parallelized on the SGI ORIGIN2000 cluster at Institute of Fluid Science, Tohoku University, by distributing flow analyses of design

candidates to 64 processing elements. The present method successfully obtained a design that reduced entropy production by more than 19% compared with the rotor67 while satisfying constraints on the mass flow rate and the pressure ratio. The use of the present tool for turbomachinery blade design is demonstrated to allow designers to achieve higher aerodynamic efficiency, while shortening design cycle and reducing design costs significantly.

INTRODUCTION

Aircraft industry is increasingly exposed to considerable commercial competitions to reduce operation costs and to increase safety. Key factors for success in developing an aircraft are reduction in cost, timeliness, and improvement in quality of the

* NRC Research Associate, Turbomachinery and Propulsion System Division, Member AIAA. Located at Ohio Aerospace Institute ICOMP, 22800 Cedar Point Rd., Cleveland, OH 44142, USA

† Senior Scientist, Turbomachinery and Propulsion System Division, Associate Fellow AIAA

Associate Professor, Institute of Fluid Science, Associate Fellow AIAA

Copyright © 2002 by the American Institute of Aeronautics and Astronautics, Inc. No copyright is asserted in the United States under Title 17, U.S. Code. The U.S. Government has a royalty-free license to exercise all rights under the copyright claimed herein for governmental purposes. All other rights are reserved by the copyright owner.

product. Among many components of an aircraft, design of jet engines is critical because a small improvement in efficiency can result in huge savings for commercial airlines in yearly fuel costs. Computational design tool offers a feasible approach to solving a very complex nonlinear optimization problem involving a multitude of design variables and constraints in a systematic and efficient manner that is impossible to do otherwise. Application of this computational design optimization approach to compressor and turbine blade designs can reduce design cost, design cycle, as well as increase efficiency of jet engines.

With advances in Computational Fluid Dynamics (CFD) and computer hardware, CFD has become an integral part of the blade design process. CFD has been employed to cut aerodynamic design cost and time scales by reducing the number of required experiments. However, the current design process is, by and large, still based on trial and error, and the success of the final design depends on the designer's expertise and company's proprietary database. CFD technology will be able to display its ability to the full extent when it is coupled with a numerical optimization method and when any human interactions in the design procedure are minimized.

Numerical optimization methods have been successfully used for a variety of design problems. However, application to aerodynamic blade shape optimization problem still remains as a formidable challenge. First of all, flow field inside a transonic compressor or turbine is highly three-dimensional and extremely complex. Therefore three-dimensional Navier-Stokes computations are essential for aerodynamic blade shape optimization. The section-by-section or quasi-3D technique is more efficient computationally, but has limitations in capturing 3D effects. On the other hand, design optimization based on three-dimensional Navier-Stokes is computation-intensive and currently still expensive.

Second reason is that aerodynamic design optimization problem of a blade itself is very hard to solve. Because aerodynamic performance of a transonic blade is very sensitive to its shape, a blade shape must be parameterized with a large number of parameters to be optimized. In addition, objective function landscape of an aerodynamic design optimization problem is often multimodal and nonlinear because the flow field is governed by a system of nonlinear partial differential equations. Finally, aerodynamic blade shape optimization problem is usually subject to some required constraints, such as mass flow rate, pressure ratio, and others.

The gradient-based methods are a well-known optimization algorithm in which the optimum is

probed by calculating the local gradient information. These methods are efficient in searching an optimum, especially when it is isolated. The optimum obtained from these methods will be a global one, if the objective and constraints are differentiable and convex. Therefore, this approach has been widely used for many design problems including aerodynamic designs such as wing design¹, scramjet nozzle design², supersonic wing-body design³, and more complex aircraft configurations^{4,5}. This approach has been also applied to aerodynamic design optimization problems of turbomachinery such as vaneless diffuser for a centrifugal compressor⁶ and compressor airfoils⁷. However, distribution of an objective function of an aerodynamic design problem is usually multimodal, and thus, one could only hope for a local optimum neighboring the initial design point by using the gradient-based methods. To find a global optimum, one must start the optimization process repeatedly from a number of initial points and check for consistency of the optima obtained. In this sense, the gradient-based methods are neither efficient nor robust.

Evolutionary Algorithms (EAs) are emergent optimization algorithms mimicking mechanism of the natural evolution, where a biological population evolves over generations to adapt to an environment by selection, recombination and mutation. When EAs are applied to optimization problems, fitness, individual and genes usually correspond to an objective function value, a design candidate, and design variables, respectively. One of the key features of EAs is that they search simultaneously from multiple points in the design space, instead of moving from a single point like gradient-based methods do. Furthermore, these methods work on function evaluations alone and do not require derivatives or gradients of the objective function. These features lead to the advantages such as robustness, suitability to parallel computing and simplicity in coupling the CFD code with other disciplines codes. Owing to these advantages over the analytical methods, EAs have become increasingly popular in a broad class of design problems (for example, see [8,9]). EAs have been also successfully applied to aerodynamic shape optimization problems such as airfoil shape design¹⁰⁻¹², Multi-element airfoil shape design¹³, subsonic to supersonic wing shape designs¹⁴⁻¹⁶, vaned diffuser design for centrifugal compressor¹⁷, compressor airfoil design¹⁸ and turbine airfoil design¹⁹.

The objective of the present study is to develop a reliable and efficient design optimization tool for transonic compressor blade shape design optimization problems. A real-coded Adaptive-Range

Genetic Algorithm (real-coded ARGAs) is used for design optimization. To represent flow fields accurately and produce reliable designs, three-dimensional Navier-Stokes computation is used for aerodynamic analysis. To reduce turn-around time, the computation is parallelized on the SGI ORIGIN2000 cluster at the Institute of Fluid Science, Tohoku University of Japan, by distributing flow analyses of design candidates to 64 processing elements. The present method is applied to aerodynamic redesign of NASA rotor67²⁰.

THREE-DIMENSIONAL NAVIER-STOKES SOLVER FOR CASCADE FLOW

Flow field inside high-speed axial-flow turbomachinery is highly three-dimensional and involves significant viscous effects, such as boundary-layer separations and shock wave/boundary layer interactions. Therefore three-dimensional Navier-Stokes computations are essential for blade shape optimization because further improvement in the aerodynamic performance requires detailed knowledge of the flow structure such as secondary flows and tip clearance flow.

In this study, the three-dimensional Navier-Stokes code TRAF3D^{21,22} is used for aerodynamic analysis of blade designs. Capability of the present code has been validated by comparing the computed results to some experiments such as the Goldman annular vane with and without end wall contouring, the low speed Langston linear cascade²¹ as well as the NASA rotor67²².

The present code solves the three-dimensional full Reynolds-averaged Navier-Stokes equations. The present code uses a central-differencing scheme including artificial dissipation terms introduced by Jameson, Schmidt, and Turkel²³ to maintain stability and to prevent oscillations near shocks or stagnation points. In order to minimize the amount of artificial diffusion inside the shear layer, the eigenvalues scaling of Martinelli²⁴ and Swanson and Turkel²⁵ are used. The two-layer eddy-viscosity model of Baldwin and Lomax is used for the turbulence closure. The system of the differential equations is advanced in time using an explicit four-stage Runge-Kutta scheme. In order to accelerate convergence of calculations, local time-stepping, implicit residual smoothing²⁶, and the Full Approximation Storage (FAS) multigrid technique²⁷ are used.

At the subsonic axial inlet, the flow angles, total pressure and total enthalpy are specified according to the theory of characteristics while the outgoing Riemann invariant is taken from the interior. At the subsonic axial outlet, the average value of the static pressure at the hub is prescribed and the density and components of velocity are extrapolated together

with the circumferential distribution of pressure. The radial equilibrium equation is used to determine the spanwise distribution of the static pressure. On sidewalls, the momentum equation, the no-slip condition, and the temperature condition are used to compute pressure and density. For the calculations presented in this paper, all the walls have been assumed to be adiabatic. The periodicity from blade passage to blade passage is imposed by setting periodic phantom cell values. At the wake, where the grid is not periodic, the phantom cells overlap the real ones. Linear interpolations are then used to compute the value of the dependent variables in phantom cell.

The three-dimensional grids are obtained by stacking two-dimensional grids generated on the blade-to-blade surface. These two-dimensional grids are of C-type and are elliptically generated, with controlled grid spacing and orientation at the wall. The problem of grid skewness due to high stagger or large camber is addressed by allowing the grid to be non-periodic on the wake²⁸. By adding lines near the wall, viscous grids are obtained from the inviscid grids. The wall normal spacing scaled with the axial chord is 10^{-4} . In the spanwise direction a standard H-type structure has been adopted. Near the hub and tip walls geometric stretching is used for a specified number of grid points, after which the spanwise spacing remains constant. The number of the grid points is 201 chordwise x 53 tangential x 57 spanwise. Among the 201 chordwise grid points, 149 grid points are distributed along the blade shape. The computational grid for NASA rotor67 is shown in Fig. 1.

BLADE SHAPE PARAMETERIZATION

Here a rotor blade shape is represented by four blade profiles, respectively at 0%, 31%, 62%, and 100% spanwise stations (all spanwise locations discussed here are measured from the hub) and linearly interpolated. Each of these sectional profiles can be uniquely defined by using a mean camber line and a thickness distribution and they are parameterized by the third-order B-Spline curves. Parameterization using B-Spline curves is one of the most popular approaches for airfoil designs.

When B-Spline curves are used for shape parameterization, positions of control points of the B-Spline curves are often considered as the design parameters. Here, five control points are used for the mean camber line as illustrated in Fig 2. For the thickness distribution, two control points are added at the leading edge and the trailing edge so that these points represent leading edge and trailing edge radii, respectively. Chordwise locations of the control points at leading edge and trailing edge are frozen to

zero and one, respectively. As a result, 14 design parameters are required to represent a sectional shape. Each blade shape is then represented with 56 design parameters.

EVOLUTIONARY ALGORITHM

EAs mimic mechanism of natural evolution, where a biological population evolves over generations to adapt to an environment by selection according to fitness, recombination and mutation of genes (Fig. 3). In EAs, a design candidate, objective function values, and design variables usually correspond to an individual, fitness, and genes, respectively.

Starting with an initial population of design candidates that is often generated by random sampling from the design space, EAs select good design candidates in terms of fitness, which is assigned on the bias of their objective function values. Typically, fitness of a design candidate is its objective function value itself for a single objective problem. Recombination is applied, where new population is generated by exchanging features of the selected designs with the intent of improving the fitness of the next generation. Then, mutation is applied to design parameters of the new population to maintain diversity in the population.

One of the key features of EAs is that it searches from multiple points in the design space in contrast to the traditional methods that usually move from a single design point. In addition, EAs use objective function values alone to determine a search direction and do not require gradients of the objective function while the traditional methods use local gradient information of an objective function. These features also lead to advantages such as,

1) Robustness: Deterministic methods, such as the gradient-based methods, typically start with a single design point and use the local gradient information to determine a search direction. As a result, they generally lead to a local, not necessarily a global optimum near the starting point. In contrast to them, EAs determine their search direction globally and probabilistically but efficiently using their unique operators so-called recombination and mutation that give EAs capability of finding global optimum. Compared with other probabilistic methods such as the simulated annealing method²⁹ that is similar to the gradient-based methods but tries a random step according to the so-called Boltzmann probability distribution, EAs are more robust because they maintain a population of design candidates and they don't use function gradients that direct the search toward a local optimum. In addition, EAs have a capability to handle any design problems that may involve

non-differentiable objective function and/or a mix of continuous, discrete, and integer design parameters.

- 2) Suitability to parallel computing: Because EAs are population-based search algorithms, all design candidates in each generation can be evaluated in parallel by using the simple master-slave concept. Parallel efficiency is extremely high, if objective function evaluations consume most of the computational time. Aerodynamic design optimization is a typical case.
- 3) Simplicity in coupling evaluation codes: Because EAs use only objective function values of design candidates, EAs do not need substantial modification or sophisticated interface to evaluation codes. If an all-out re-coding were required to every optimization problem, extensive validation of the new code would be necessary every time. EAs can save such troubles.
- 4) Straightforward application to multiobjective optimization problems: Because EAs maintain multiple designs, EAs can find compromised optimum designs, so-called Pareto-optimal solutions, by introducing Pareto-optimal concept.

In the present study, the real-coded Adaptive-Range Genetic Algorithm³⁰ (real-coded ARGAs) is used. The real-coded ARGAs is an EA that can solve large-scale design optimization problems very efficiently by promoting the population toward promising design regions during the optimization process.

To represent design parameters of design candidates, the floating-point representation³¹ is used where an individual is characterized by a vector of real numbers. It is natural to use the floating-point representation for real parameter optimization problems instead of binary representation, because it is conceptually closest to the real design space, and moreover, the string length is reduced to the number of design variables.

The parental selection consists of the stochastic universal sampling³² and the ranking method³¹. To handle design constraints, the constrained domination approach³³ is used. Blended crossover³⁴ (BLX-0.5) is used for recombination. Mutation takes place at a probability of 10% and then adds a random disturbance to the corresponding gene. The present EA adopts the elitist strategy³⁵ where the best and the second best individuals in each generation are transferred into the next generation without any recombination or mutation. Population size is set to 64.

The main concern related to the use of a three-dimensional Navier-Stokes solver for aerodynamic shape design is the required computational effort.

Fortunately, powerful parallel computers are increasingly made available in many institutions and universities. In addition, EAs are intrinsically amenable to parallel algorithms and the computation can be easily parallelized. Furthermore, the PC clusters are emerging as a powerful and affordable alternative. Hence, the issue of computational cost is rapidly diminishing and yet, the ability of applying the EAs to complex problems is increasing. In the present study, all computations are performed on the SGI Origin2000 cluster consisting of 640 processing elements located at the Institute of Fluid Science, Tohoku University in Japan. The total scalar performance and the total memory size are 384GLOPS and 640GB, respectively.

Here aerodynamic evaluation of design candidates at each generation is parallelized using the simple master-slave concept; the grid generations and the flow calculations associated to the design candidates of a generation are distributed into 64 processing elements of the SGI Origin2000 cluster. This makes the corresponding turnaround time almost 1/64 of that needed on a single processor alone, because the computational time used for EA operators are negligible compared with that of Navier-Stokes computations.

DESIGN OPTIMIZATION PROBLEM

The optimization problem considered here is to seek a redesign of NASA rotor67²⁰. The rotor is a low-aspect-ratio transonic axial-flow fan rotor and is the first-stage rotor of a two-stage fan. The rotor design pressure ratio is 1.63 at a mass flow of 33.25 kg/sec. The design rotational speed is 16043 rpm, which yields a tip speed of 429 m/sec and an inlet tip relative Mach number of 1.38. The rotor has 22 blades and aspect ratio of 1.56 (based on average span/root axial chord). The rotor solidity varies from 3.11 at the hub to 1.29 at the tip. The inlet and exit hub/tip radius ratios are 0.375 and 0.478, respectively. Reynolds number is 1.797M based on the blade axial chord at the hub.

The objective of aerodynamic rotor shape design optimization problem is to minimize the flow loss manifested via entropy generation. To achieve this goal, the isentropic efficiency is often considered as a design objective function to be maximized. From our experience, however, a numerical design optimization using the evolutionary algorithm coupled with the three-dimensional Navier-Stokes solver resulted in an optimum design that maximized its isentropic efficiency by maximizing the total pressure ratio rather than minimizing flow loss. Therefore, mass-weighted sum of entropy production from inlet to exit at the design point of rotor67 is considered as the objective function to be minimized.

Because an optimized rotor design should meet the required mass flow rate and pressure ratio, they are maintained by specifying constraints on them:

$$\left| \frac{\text{massflowrate}_{\text{design}} - \text{massflowrate}_{\text{rotor67}}}{\text{massflowrate}_{\text{rotor67}}} \right| \leq 0.005 \quad (1)$$

$$\left| \frac{\text{pressureratio}_{\text{design}} - \text{pressureratio}_{\text{rotor67}}}{\text{pressureratio}_{\text{rotor67}}} \right| \leq 0.01 \quad (2)$$

These constraints are satisfied by using the constrained domination approach³³.

RESULTS

The first step of the EA is to properly define the initial design space. The existing design (rotor67) is used as a baseline around which the initial candidates are populated. Specifically, the central values of the initial design space are made to correspond to the design parameter values representing the rotor67 geometry. These values are found by minimizing geometry difference from rotor67 by using the EA without any flow computation. Unbiased initial population is generated by randomly spreading solutions over the entire initial design space. Population size and number of generation are 64 and 200, respectively. The computation is parallelized on 64 processing elements of the SGI Origin2000 cluster. The computational time is about 7 hours, where most of the computational time is spent on grid generation.

Optimization history in terms of objective function value (entropy production) is shown in Fig. 4. Entropy production was reduced from the original design by more than 19% after 100 generations. Better designs may be obtained if the computation is further continued. At each generation, 64 Navier-Stokes computations were performed in parallel using 64 processing elements of the SGI ORIGIN2000 cluster. Parallelization efficiency was almost 1 because computational time necessary for the real-coded ARGAs is negligible. Each Navier-Stokes computation took about 16 hours of computational time on one SGI ORIGIN2000 processing element while the real-coded ARGAs used less than one second per each generation. The total turn around time was about 1550 hours (about two months). Table 1 presents performance of the optimum design and rotor67. The constraints on the mass flow rate and pressure ratio are satisfied. The isentropic efficiency is improved by 1.783%, resulting in a higher pressure ratio across the rotor than the baseline design. The blade profiles of the optimized design and rotor67 are shown in Fig. 5.

Figure 6 compares spanwise entropy production

distributions of rotor67 and the optimum design. The figure shows that the optimized design reduced entropy production in the regions between the hub and the midspan and near the tip.

Figures 7-10 compare blade profiles and surface static pressure distributions at 10%, 33%, 67%, and 90% spanwise stations, respectively. Excessive flow accelerations near the leading edge at 10% and 33% spans are diminished by increasing the incidence angles. In addition, at the 67% and 90% stations, the shock on the suction side moves toward aft and considerably weakens due to the aft movement of the maximum camber position. Figures 11-14 present the corresponding relative Mach number contours. The optimized design avoids supersonic bubble on the suction side near the leading edge at 10% span. The supersonic bubble at 33% is also minimized. This explains the reduction in entropy production between the hub and the midspan. At 67% and 90% stations, the bow shock impinging the blade suction side and its reflection shock have become more oblique and are significantly weakened to reduce entropy production through the shocks. Also, flow separation is decreased due to a weakened shock, thus contributing to a reduction of entropy generation.

Figures 15 and 16 show the oil flow patterns and static pressure contours of rotor67 and the optimized design on pressure and suction surfaces, respectively. The figures show that the shock wave on the suction side of the optimized design is weakened and more oblique than that of rotor67 in the meridional plane as well as in the tangential plane as shown in the Figs. 13 and 14, to reduce the shock-generated entropy.

Figure 17 shows the performance maps of the optimum design and rotor67. Although optimization is carried out for the designed operating condition (33.774kg/sec), it is remarkable that the optimized design still maintains higher isentropic efficiency over the entire range of operating conditions, from the choke to stall limits.

CONCLUSIONS

A reliable and efficient aerodynamic design optimization tool for transonic compressor blade has been developed. The real-coded ARGAs were used for efficient and robust design optimization. To represent flow fields accurately and produce reliable designs, a three-dimensional Navier-Stokes solver was used for aerodynamic analysis.

To ensure feasibility of the present method, aerodynamic redesign of the NASA rotor67 was demonstrated. Entropy production was considered as the objective function to be minimized in order to reduce flow losses at the rotor. The code was parallelized and the computation was run on the SGI

ORIGIN2000 cluster at the Institute of Fluid Science by using the simple master-slave concept. The total turn around time was about 1550 hours. The present method successfully obtained a design that reduced entropy production by more than 19% compared with the rotor67 while satisfying constraints on the mass flow rate and the pressure ratio. This study demonstrated that the present method offers a promising approach to turbomachinery designer to design a better machine, while shortening design cycle and reducing design costs.

ACKNOWLEDGEMENTS

The authors thank Drs. L. M. Larosiliere and R. V. Chima at NASA Glenn Research Center for their valuable advices in defining the present design optimization problem, and Dr. E. R. McFarland for managing the project. The authors also thank Dr. M. Marconcini at University of Florence for his help in using the TRAF3D code. The generosity of Advanced Fluid Information Research Center at Tohoku University for providing computational time on the SGI ORIGIN2000 cluster is greatly appreciated.

REFERENCES

- 1) Hicks, R. M. and Henne, P. A., "Wing Design by Numerical Optimization," *Journal of Aircraft*, Vol. 15, 1978, pp.407-412.
- 2) Baysal, O. and Eleshaky, M. E., "Aerodynamic Design Optimization Using Sensitivity Analysis and Computational Fluid Dynamics," *AIAA Journal*, Vol. 30, No. 3, 1992, pp. 718-725.
- 3) Reuther J. J. and Jameson, A., "Supersonic wing and wing-body shape optimization using an adjoint formulation," Technical report, The Forum on CFD for Design and Optimization, (IMECE95), San Francisco, California, November 1995.
- 4) Reuther, J. J., Jameson, A., Alonso, J. J., Rimlinger, M. J. and Saunders, D., "Constrained Multipoint Aerodynamic Shape Optimization Using an Adjoint Formulation and Parallel Computers, Part 1," *Journal of Aircraft*, Vol.36, No. 1, January-February 1999, pp.51-60.
- 5) Reuther, J. J., Jameson, A., Alonso, J. J., Rimlinger, M. J. and Saunders, D., "Constrained Multipoint Aerodynamic Shape Optimization Using an Adjoint Formulation and Parallel Computers, Part 2," *Journal of Aircraft*, Vol.36, No. 2, January-February, 1999, pp.61-74.
- 6) Lee, Y.-T., Luo, L., and Bein, T. W., "Direct Method for Optimization of a Centrifugal Compressor Vaneless Diffuser," *Journal of Turbomachinery*, Vol.123, January 2001, pp.73-80

- 7) Koller, U, Monig, R., Kusters, B., and Schreiber, H.-A., "Development of Advanced Compressor Airfoils for Heavy-Duty Gas Turbines – Part I: Design and Optimization," *Journal of Turbomachinery*, Vol. 122, July 2000, pp.397-405.
- 8) Miettinen, K., Makela, M. M., Neittaanmaki, P. and Periaux, J. (eds.), *Evolutionary Algorithms in Engineering and Computer Science*, John Wiley & Sons Ltd, Chichester, U.K., 1999, Chaps.17-24.
- 9) Dasgupta, D. and Michalewicz, Z. (eds.), *Evolutionary Algorithms in Engineering Applications*, Springer-Verlag, Berlin, Heidelberg, 1997.
- 10) Quagliarella, D. and Cioppa, A. D., "Genetic Algorithms applied to the Aerodynamic Design of Transonic Airfoils," AIAA-94-1896-CP, June 1994.
- 11) Yamamoto, K. and Inoue, O., "Applications of Genetic Algorithm to Aerodynamic Shape Optimization," AIAA Paper 95-1650-CP, A collection of technical papers, 12th AIAA Computational Fluid Dynamics Conference, CP956, San Diego, CA, June 1995, pp. 43-51.
- 12) Poloni, C., Mosetti, G. and Contessi, S., "Multi Objective Optimization by GAs: Application to System and Component Design," Proceedings of the Third ECCOMAS Computational Fluid Dynamics Conference, John Wiley & Sons, Ltd, Chichester, U.K., 1996, pp. 258-264.
- 13) Cao, H. V. and Blom, G. A., "Navier-Stokes/Genetic Optimization of Multi-Element Airfoils," AIAA 96-2487, June 1996.
- 14) Obayashi, S. and Oyama, A., "Three-Dimensional Aerodynamic Optimization with Genetic Algorithms," Proceedings of the Third ECCOMAS Computational Fluid Dynamics Conference, John Wiley & Sons, Ltd, Chichester, U.K., 1996, pp.420-424.
- 15) Oyama, A., "Multidisciplinary Optimization of Transonic Wing Design Based on Evolutionary Algorithms Coupled with CFD solver," CD-ROM Proceedings of the ECCOMAS 2000, 2000.
- 16) Sasaki, D., Obayashi, S., Sawada, K. and Himeno, R., "Multiobjective Aerodynamic Optimization of Supersonic Wings Using Navier-Stokes Equations," CD-ROM Proceedings of the ECCOMAS 2000, 2000.
- 17) Benini, E. and Tournlidakis, A., "Design Optimization of Vaned Diffusers for Centrifugal Compressors Using Genetic Algorithms," AIAA Paper 2001-2583, 2001.
- 18) Uelschen, M. and Lawrenz, M., "Design of Axial Compressor Airfoils With Artificial Neural Networks and Genetic Algorithms," AIAA Paper 2000-2546, 2001.
- 19) Akmandor, S. and Oksuz, O., "Aerodynamic Optimization of Turbomachinery Cascades Using Euler/Boundary-Layer Coupled Genetic Algorithms," AIAA Paper 2001-2577, 2001.
- 20) Walter, S. C., William, S., and Donald, C. U., "Design and Performance of a 427-Meter-Per-Second-Tip-Speed Two-Stage Fan Having a 2.40 Pressure Ratio," NASA TP-1314, October 1978.
- 21) Arnone, A., Liou, M.-S., and Povinelli, L. A., "Multigrid Calculation of Three-Dimensional Viscous Cascade Flows," NASA TM-105257, ICOMP-91-18, 1991.
- 22) Arnone, A., "Viscous Analysis of Three-Dimensional Rotor Flow Using a Multigrid Method," *ASME Journal of Turbomachinery*, Vol. 116, July 1994, pp. 435-445.
- 23) Jameson, A., Schmidt, W., and Turkel, E., "Numerical Solutions of the Euler Equations by Finite Volume Methods Using Runge-Kutta Time-Stepping Schemes," AIAA paper 81-1259, 1981.
- 24) Martinelli, L. and Jameson, A., "Validation of a Multigrid Method for the Reynolds Averaged Equations," AIAA paper 88-0414, 1988.
- 25) Swanson, R. C., and Turkel, E., "Artificial Dissipation and Central Difference Schemes for the Euler and Navier-Stokes Equations," AIAA paper 87-1107, 1987.
- 26) Jameson, A., "The Evolution of Computational Methods in Aerodynamics," *Journal of Appl. Mech.*, Vol. 50, 1983.
- 27) Jameson, A., "Transonic Flow Calculations," MAE Report 1651, MAE Department, Princeton University, July 1983.
- 28) Arnone, A., Liou, M.-S., and Povinelli, L. A., "Transonic Cascade Flow Calculations Using Non-Periodic C-Type Grids," Computational Fluid Dynamics Symposium on Aeropropulsion, NASA Lewis Research Center, Cleveland, April, 1990.
- 29) Aarts, E. and Korst, J., *Simulated Annealing and Boltzmann Machines*, John Wiley & Sons, Chichester, U.K., 1989.
- 30) Oyama, A., Obayashi, S., and Nakahashi, K., "Wing Design Using Real-Coded Adaptive Range Genetic Algorithm," 1999 IEEE International Conference on Systems, Man and Cybernetics, Tokyo, Japan, 1999.
- 31) Michalewicz, Z., "Genetic Algorithms + Data Structures = Evolution Programs," third revised edition, Springer-Verlag, Berlin, 1996.
- 32) Baker, J. E., "Reducing Bias and Inefficiency in the Selection Algorithm," Proceedings of the Second International Conference on Genetic

Algorithms, Morgan Kaufmann Publishers, Inc., San Mateo, California, 1987, pp 14-21.

- 33) Deb, K., Pratap, A. and Moitra, S., "Mechanical Component Design for Multiple Objectives Using Elitist Non-Dominated Sorting GA," *Lecture Notes in Computer Science 1917 Parallel Problem Solving from Nature – PPSN VI*, edited by Schoenauer, M., Deb, K., Rudolph, G., Yao, X., Lutton, E., Merelo, J. J., and Schwefel, H.-P., Springer, Berlin, Germany, 2000, pp.859-868.
- 34) Eshelman, L. J. and Schaffer, J. D., "Real-Coded Genetic Algorithms and Interval Schemata," *Foundations of Genetic Algorithms.2*, Morgan Kaufmann Publishers, Inc., San Mateo, California, 1993, pp 187-202.
- 35) De Jong, K. A., "An Analysis of the Behavior of a Class of Genetic Adaptive Systems," Doctoral Dissertation, University of Michigan, Ann Arbor, 1975.

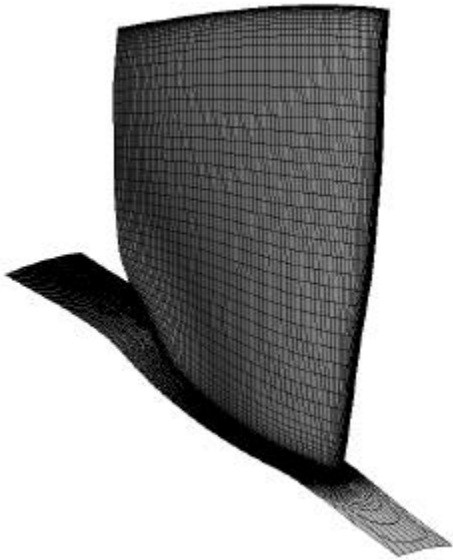


Figure 1. Computational grid over NASA rotor67.

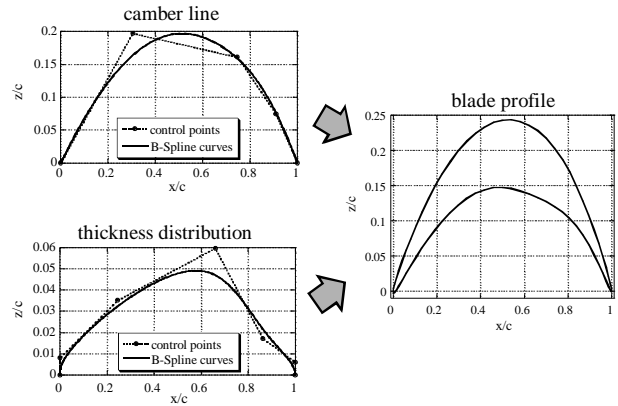


Figure 2. B-Spline curves for mean camber line and thickness distribution and the resultant blade profile.

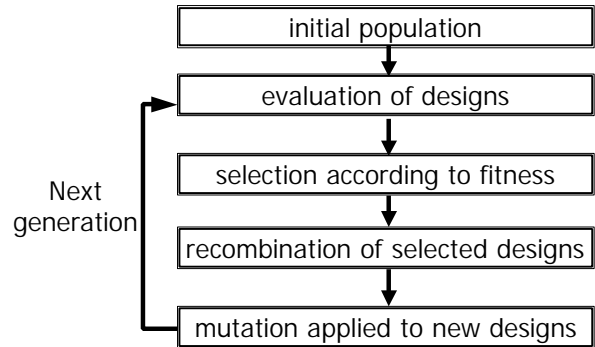


Figure 3. Flowchart of typical evolutionary algorithms.

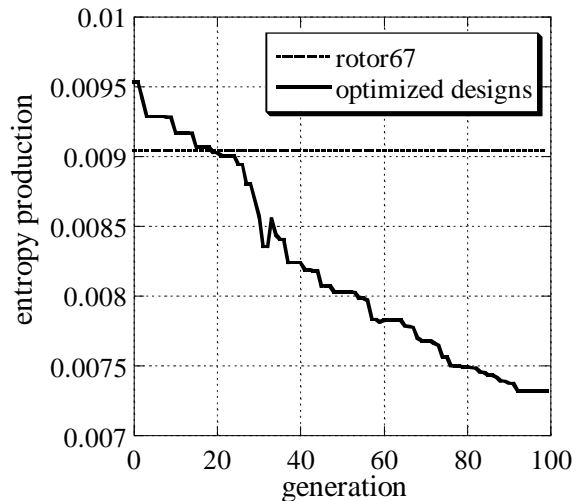


Figure 4. Optimization history in terms of entropy production.

Table 1. Computed performance of rotor67 and the optimum design.

	mass flow [kg/sec]	isentropic efficiency	pressure ratio	entropy production
Rotor67	33.774	0.91890	1.6758	0.0090467
Optimum	33.929	0.93528	1.6859	0.0073263

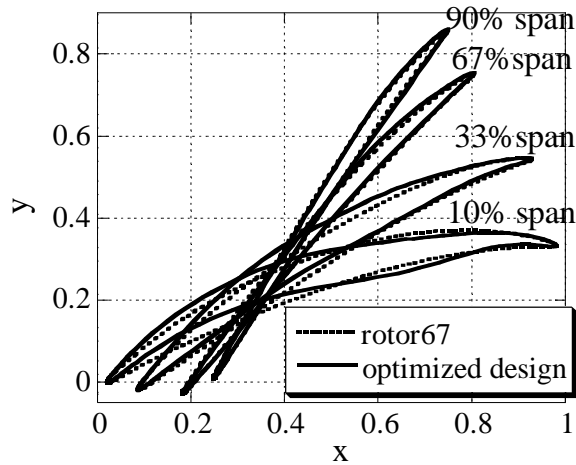


Figure 5. Blade profiles of the optimum design and rotor67.

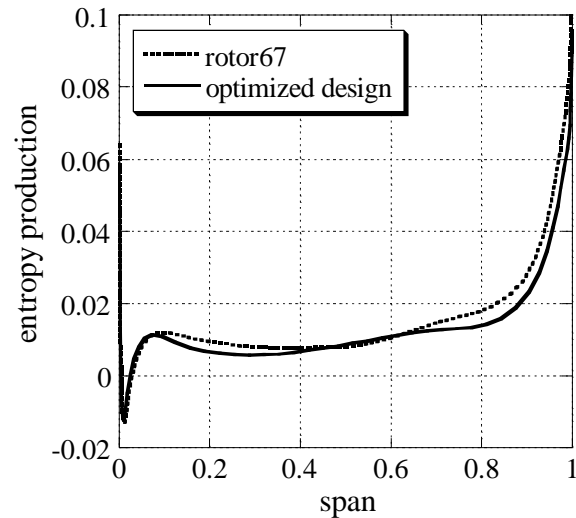


Figure 6. Comparison of spanwise entropy production distribution.

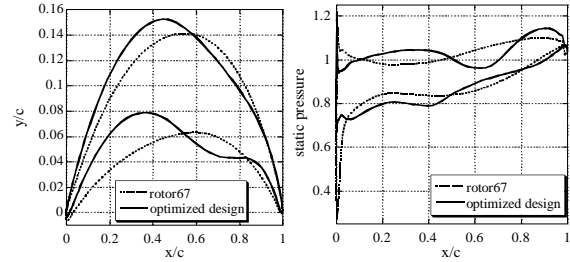


Figure 7. Comparison between the optimum design and rotor67 at 10% span.

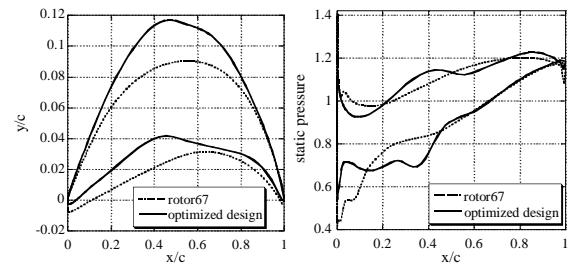


Figure 8. Comparison between the optimum design and rotor67 at 33% span.

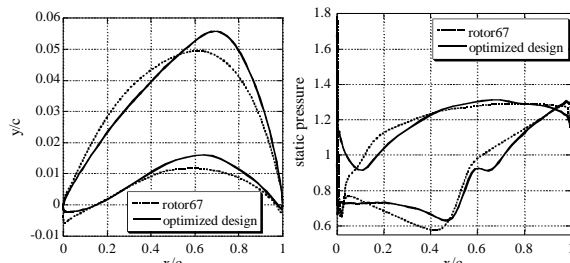


Figure 9. Comparison between the optimum design and rotor67 at 67% span.

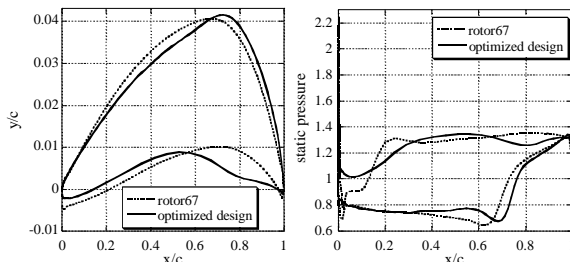


Figure 10. Comparison between the optimum design and rotor67 at 90% span.

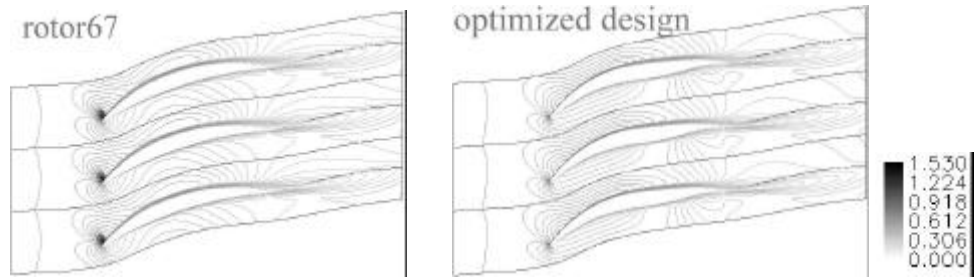


Figure 11. Relative Mach number contours of the optimum design and rotor67 at 10% span.

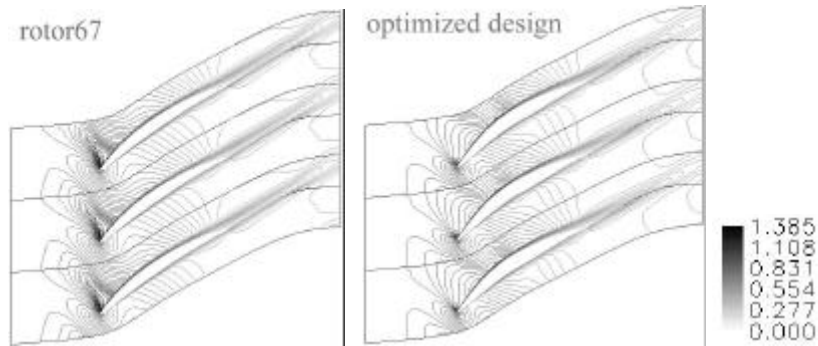


Figure 12. Relative Mach number contours of the optimum design and rotor67 at 33% span.

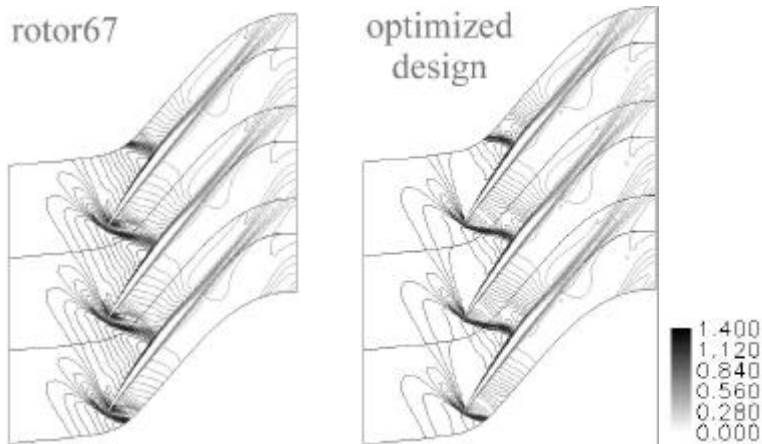


Figure 13. Relative Mach number contours of the optimum design and rotor67 at 67% span.

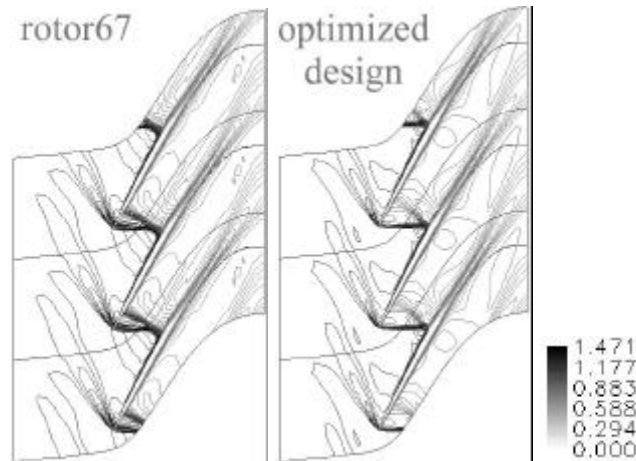


Figure 14. Relative Mach number contours of the optimum design and rotor67 at 90% span.

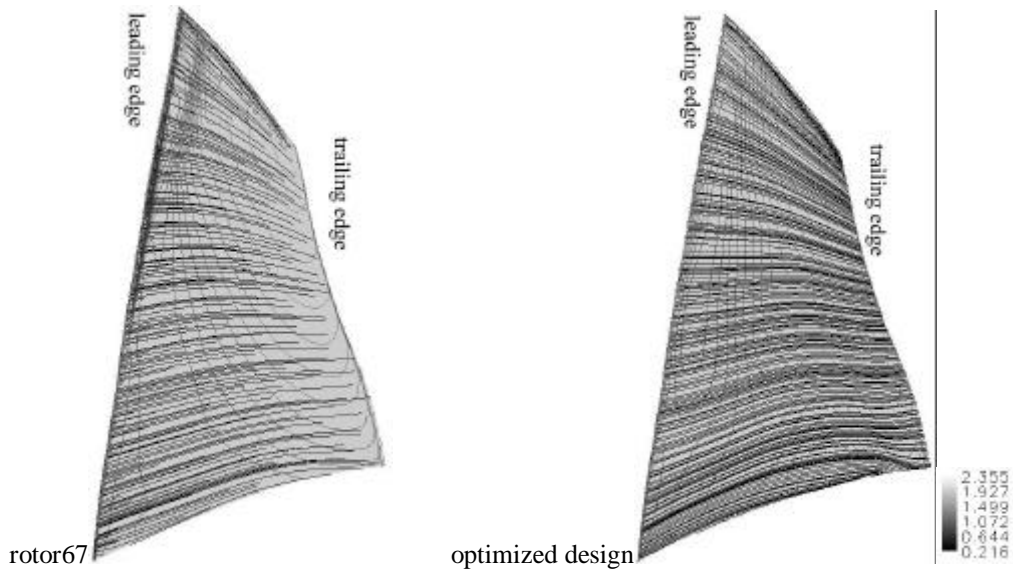


Figure 15. Oil flow patterns and static pressure contours on pressure surfaces.

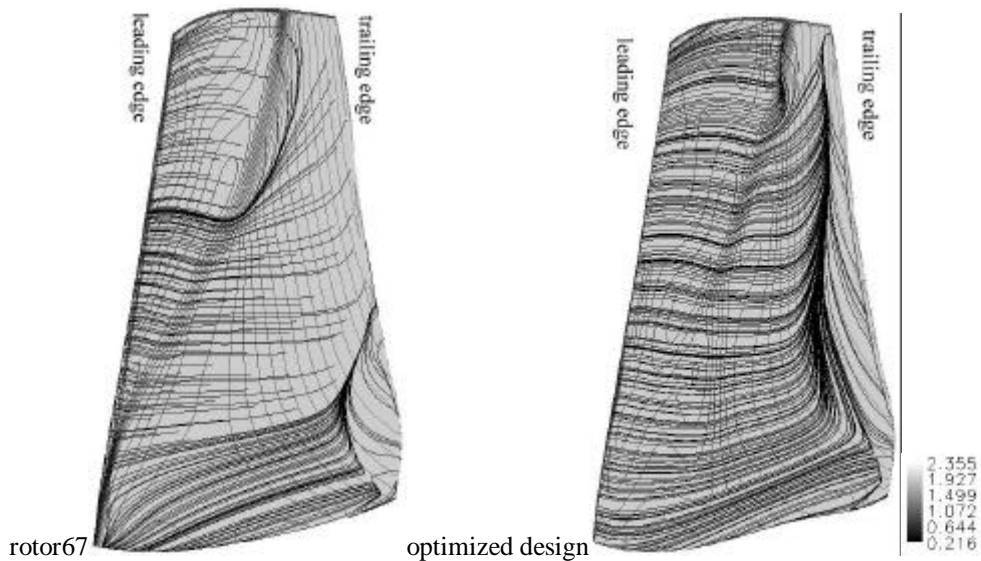


Figure 16. Oil flow patterns and static pressure contours on suction surfaces.

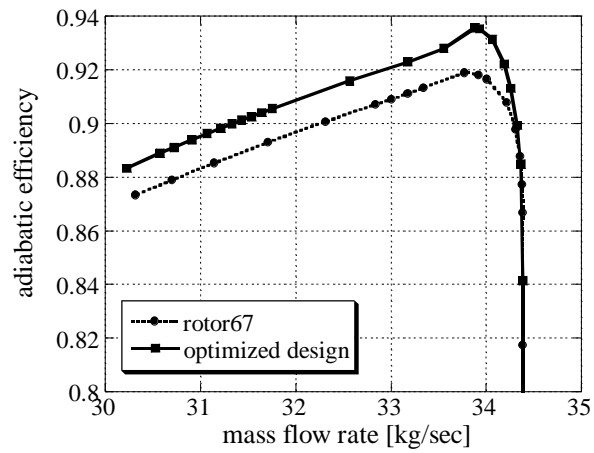


Figure 17. Performance map comparison between rotor67 and the optimum design.